Investigating Grain Boundaries in $BaCuS_{1-x}Se_xF$ Using Impedance Spectroscopy

Author:
Briony Horgan
Physics Department
Oregon State University

Advisor:
Dr. Janet Tate
Physics Department
Oregon State University

Submitted for review:
June 3, 2004

Impedance spectroscopy is a method of modeling materials with equivalent circuits to determine electrical properties, such as the resistivity and the dielectric constant. We explore impedance spectroscopy, both theoretically and experimentally through applying the method to samples of $BaCuS_{1-x}Se_xF$. Grain boundary effects were dominant in the results, and although they prevented us from determining the resistivity and dielectric constant of the bulk material, we gained valuable knowledge about the limits of the samples in question and limits on the impedance spectroscopy method. We discovered that although modeling the electric properties of samples with impedance spectroscopy is difficult, it is a versatile theory with many applications.

0 Contents

0.1 Table of Contents

0.2 List of Figures

1 Introduction

The goal of our project is to develop an understanding of AC impedance spectroscopy, which involves analyzing the frequency dependence of the complex impedance of a material. The hope is that it will provide a consistent and simple model for determining the electric properties of, in this instance, BaCuSF, a candidate for p-type transparent conductivity. In particular, the resistivity and the dielectric constant can be determined through this method. Resistivity can be measured by other means in our laboratory and checked against results from AC impedance spectroscopy, but the measurement of the dielectric constant would be new in our lab. The end result of the process is indeed a greater understanding of impedance spectroscopy, but also a greater appreciation for the complexities of measurements on polycrystalline samples.

Impedance spectroscopy is widely used for determining ionic conductivities, mainly for electrolytic solutions. Its application to solids has been limited, so the theory for solids exists but is somewhat incomplete in its details. The major difference between impedance spectroscopy as applied to solids versus electrolytic solutions is that the physical limits imposed by the solution (e.g. magnitude of applied voltage, applicable frequency range, etc.) do not apply to the solids – effectively, there are few or no physical limits for the materials we are interested in. The major challenge has therefore been overcoming the physical limits of our equipment, because the most interesting information is only extractable at high frequencies, voltages, etc. The most frustrating example of this is our dilemma with grain boundaries, as discussed in section 2.3.

2 Background

2.1 Modeling Impedance Responses with Basic Circuits

The response of a material to an electrical impulse can be described by a set of convenient properties, including the dielectric constant and the resistivity. The goal of impedance spectroscopy is to model a bulk material with an equivalent circuit and thereby extract these properties.

2.1.1 Basic Impedance Spectra

The basic principle of impedance spectroscopy is that any sample with a known complex impedance spectrum can be represented as some combination of resistors and capacitors that would produce the same spectrum.

In the simplest case, a sample could be represented as having only a real resistance, allowing us to model it with a resistor. The impedance of an ideal resistor is just R – ideal because we are taking R as independent of frequency. If we were to plot the impedance of a resistor as a function of frequency, the result would be a horizontal line, as shown in Fig. 2.1. Likewise, if we were to plot the real versus the imaginary impedance of a resistor on a Nyquist plot, or a plot parameterized by frequency, then all we would see is one point on the real axis, as shown in Fig. 2.2.

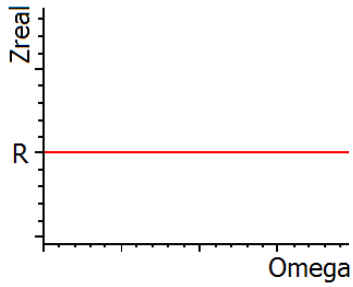

Fig. 2.1: Impedance of a resistor as a function of frequency.

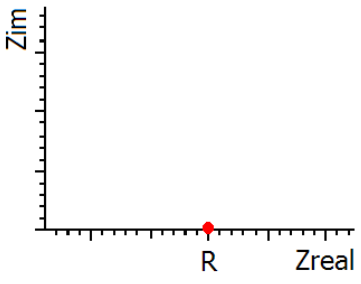

Fig. 2.2: Real v. imaginary components of a resistor's impedance.

If a sample were purely capacitive, we could represent it with an ideal capacitor. The impedance of an ideal capacitor is $(i\omega C)^{-1}$ – purely imaginary and inversely proportional to frequency, as shown in Fig. 2.3. If we were to plot the real versus the imaginary impedance of a capacitor, we would see a vertical line located on the

imaginary axis, as shown in Fig. 2.4. The magnitude of the impedance spans from infinite at direct current (frequency of zero) to zero at infinite frequency.

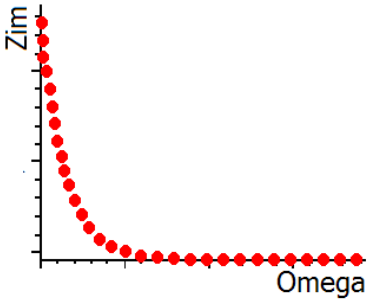

Fig. 2.3: Impedance of a capacitor as a function of frequency*.

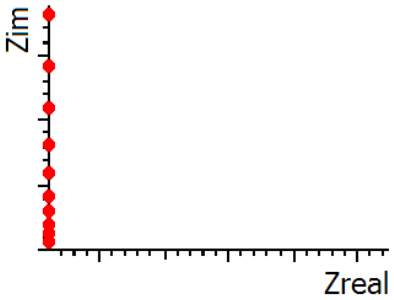

Fig. 2.4: Real v. imaginary components of a capacitor's impedance*.

If voltage is applied to a capacitive sample via metal contacts, it is likely that the contacts have an inherent resistance. We can include this effect in our model circuit by placing the resistance of the contacts in series with the capacitance of the sample, as shown in Fig. 2.5. The real and imaginary components of the impedance are the same as in Fig. 2.1 and 2.3, respectively, so the total, complex impedance is:

$$Z = R - i/\omega C. \qquad [2.1]$$

If we plot the real impedance of the circuit versus its imaginary impedance, we see a superposition of the two as a function of frequency (see Fig. 2.6).

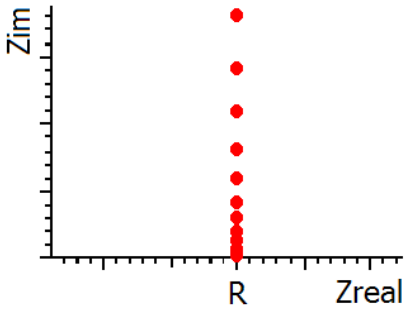

Fig. 2.6: Real vs. imaginary components of a series RC circuit's impedance.

What happens if we connect a resistor and capacitor in parallel?

*Note: The arc actually extends down from the real axis – here, and in the following plots, the imaginary impedance axis has been flipped, so all positive values are actually negative. This convention is common in impedance spectroscopy texts.

2.1.2 Parallel Circuit Impedance Spectra

Realistically, a material will nearly always have at least some bulk capacitance and some bulk resistance (even if one property dominates the other), along with some resistance due to the contacts. We can then model the material as a parallel RC circuit, as shown in Fig. 2.7, where R and C represent the bulk properties of the sample, and R_C represents the contact resistance.

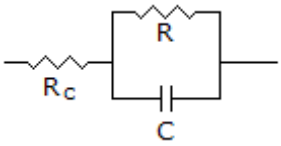

Fig. 2.7: Parallel RC circuit in series with contact resistance.

Because the current will always take the path with the lowest impedance, the total impedance for the circuit will not be as simple as the series circuit in Fig. 2.5. For this circuit:

$$Z = R_C + \frac{1}{\frac{1}{R} + i\omega C} = R_C + \frac{R}{1 + i\omega RC} = R_C + \frac{R}{1 + \omega^2 R^2 C^2} - i\frac{\omega RC}{1 + \omega^2 R^2 C^2} \qquad [2.2]^*$$

The key features of this circuit include:

- At low frequency, the resistance of the sample dominates.
- At high frequency, the capacitance of the sample dominates and effectively creates a short across the sample resistance.
- At the top of the arc, ω_0, the imaginary impedance is maximized.
- The contact resistance has the same effect on the impedance of the circuit, independent of frequency.

We can represent the effects of these characteristics mathematically by plotting the frequency dependent impedance response of this circuit on a Nyquist plot (parameterized by frequency), as shown in Fig. 2.8 and 2.9.

*Note: $Z = R_C + \frac{R}{1 + (\omega/\omega_0)^2} - i\frac{\omega/\omega_0}{1 + (\omega/\omega_0)^2} = R_C + \frac{R}{1 + (\omega/\omega_0)^2} - i\frac{1}{1 + (\omega_0/\omega)^2}$

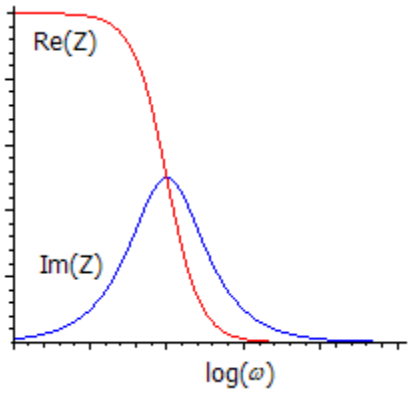

Fig. 2.8: Theoretical plot of both the real and imaginary components of the impedance for the circuit in Fig. 2.7.

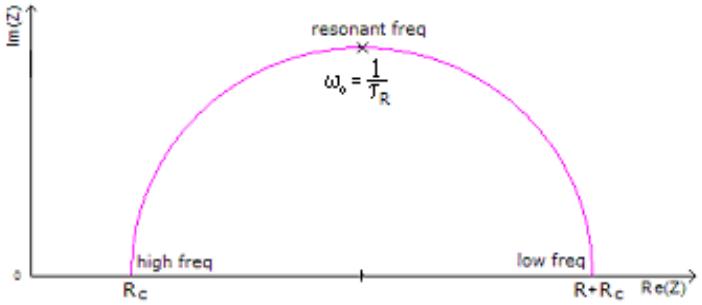

Fig. 2.9: Theoretical Nyquist plot of the complex impedance for the circuit in Fig. 2.7

If the impedance spectrum of the sample is similar to Fig. 2.8 and 2.9, the values for R and R_C can be extracted directly from the plot: the span between the arc's real intercepts gives R, while the high frequency intercept gives R_C.

The time needed for the capacitor to completely discharge through the circuit is referred to as the "relaxation time" of the circuit. For a parallel RC circuit such as in Fig. 1, $\tau_R = RC$. At the resonant frequency ω_0, $\omega_0 \tau_R = 1$, or for a parallel RC circuit, $\omega_0 = (RC)^{-1}$. Therefore, determining R and ω_0 from our data allows us to determine C as well.

2.2 Calculating Dielectric Constants and Resistivities

Now that we have a method to find R and C for the sample in question, we can use the appropriate expressions and geometry arguments to find the resistivity and dielectric constant of the bulk material. If we can approximate the sample as a geometrically simple shape such as a cylinder or cube, then both bulk quantities relate to

the sample dependent quantities through the ratio of the sample's depth L and cross-sectional area A.

The resistivity ρ is given by equation 2.3: $$\rho = R\frac{A}{L} \quad [2.3]$$

The dielectric constant ε is given by equation 2.4: $$\varepsilon = C\frac{L}{A} \quad [2.4]$$

2.3 Grain Boundary Effects

The samples we have used in our experiments are compressed powders. Because they can be more accurately represented as stacks of grains (see Fig. 2.10) than as an ideal solid, other effects can dominate the sample's bulk resistance and capacitance.

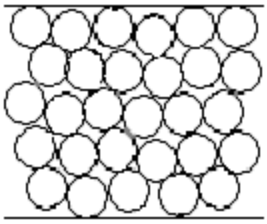

Fig. 2.10: Grains of a compressed powder material.

Oxidation of the grain exteriors creates the largest effects. The oxidized layer acts like a semiconductor, so interactions with the grain's metal interior create a boundary resistance as well as a boundary capacitance[5].

2.3.1 Brick Layer Model

The easiest way to calculate the effect of grain boundaries is to model the grains as an array of cubes[4], as shown in Fig. 2.11. The grains have a side length D and the grain boundaries a thickness d, where $d << D$. The fraction of the total volume composed of grain boundaries is then $3d/D$, or x_{gb} (we assume $x_{gi} \sim 1$). The current flow is assumed to be perpendicular to the electrodes at either end, which gives it two possible paths through each cubic grain – either through the grain *and* across one of the horizontal grain boundaries, or through the vertical grain boundaries only[3].

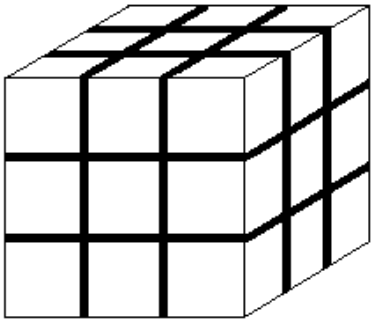

Fig. 2.11: The brick layer model for a powder such as that shown in Fig 2.10 – an array of cubic grains, separated by flat grain boundaries.

If the conductivity of the interior is much greater than that of the boundaries, the current will primarily be conducted through the smaller vertical thickness of the horizontal boundary and across the interior. Each phase (boundary or interior) acts like an independent layer of material, so the equivalent circuit model is simply two parallel RC circuits connected in series, as shown in Fig. 2.12. Because the circuits are in series, we can add their resistivities, weighted by volume[3]:

$$\rho_t = \rho_{gi} + \frac{x_{gb}}{3}\rho_{gb} \qquad [2.5]$$

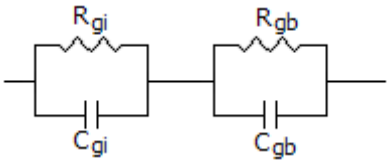

Fig. 2.12: The equivalent circuit for current conducted through the grain interior (gi) and one grain boundary (gb).

If the conductivity of the boundaries is much less than that of the interior, the current will primarily be conducted only through the vertical grain boundaries. In this case the separate sides act in parallel, so the equivalent circuit model is two parallel RC circuits connected in parallel, as shown in Fig. 2.13, which can be further reduced to one parallel RC circuit. Because the circuits are in parallel, we can add their conductivities, again weighted by volume[3]:

$$\psi_t = \psi_{gi} + \frac{2}{3}x_{gb}\psi_{gb} \qquad [2.6]$$

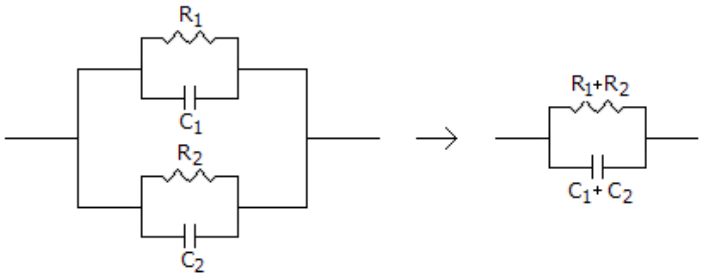

Fig. 2.13: The equivalent circuit and its reduced form for current conducted along the grain boundaries only.

Because the interior of the grains is assumed to be metallic and the exterior semiconductive, the first case ($\sigma_{gi} >> \sigma_{gb}$) is applicable to our samples. Therefore, the equivalent circuit we will use in modeling the response of our samples is that of Fig. 2.12. Using equation 2.5, the parameters of the model circuit are:

$$R_{gi} = \rho_{gi} \qquad C_{gi} = \varepsilon_{gi}$$

$$R_{gb} = x_{gb}\rho_{gi}/3 \qquad C_{gb} = 3\varepsilon_{gb}/x_{gb}$$

Dividing C_{gi} by C_{gb} gives an equation for the grain boundary volume fraction, and from that a relationship for the ratio d/D:

$$x_{gb} = 3\frac{C_{gi}}{C_{gb}}\frac{\varepsilon_{gi}}{\varepsilon_{gb}}, \quad x_{gb} = 3\frac{d}{D}$$

$$\frac{d}{D} = \frac{C_{gi}}{C_{gb}}\frac{\varepsilon_{gi}}{\varepsilon_{gb}} \qquad [2.7]$$

In practice, we can generally assume that $\varepsilon_{gb} \approx \varepsilon_{gi}$. According to Macdonald, this approximation is valid because the uncertainty it introduces is considerably less than that due to variations in *d* along the grain boundary[3]. Now we can state the capacitance of the grain interiors in terms of the capacitance of the grain boundaries:

$$\frac{d}{D} = \frac{C_{gi}}{C_{gb}} \Rightarrow C_{gi} = C_{gb}\frac{d}{D} \qquad [2.8]$$

Equation 2.8 with equation 2.4 gives the dielectric constant of the grain interior (bulk material) in terms of the sample's dimensions and the capacitance of the grain boundaries:

$$\varepsilon_{gi} = C_{gb}\frac{d}{D}\frac{A}{L} \qquad [2.9]$$

Generally, values for the grain diameter D in electroceramic materials such as $BaCuS_{1-x}Se_xF$ extend from 50-100 nm, while values for the grain boundary depth d vary between 1 and 10 nm.[7] These values give a range for the d/D correction factor of 10^{-2} to 0.2.

2.3.2 Grain Boundary Nyquist Plots

If we include grain boundary effects and contact resistance in the model of our sample, we must apply the circuit (derived in section 2.3.1) shown in Fig. 2.14. The impedance for such a circuit can be calculated simply by adding the boundary and interior impedances, both of the form of equation 2.2:

$$Z = R_C + \frac{R_{gb}}{1+\omega^2 R_{gb}^2 C_{gb}^2} + \frac{R_{gi}}{1+\omega^2 R_{gi}^2 C_{gi}^2} - i\left[\frac{\omega R_{gi} C_{gi}}{1+\omega^2 R_{gi}^2 C_{gi}^2} + \frac{\omega R_{gb} C_{gb}}{1+\omega^2 R_{gb}^2 C_{gb}^2}\right] \quad [2.10]$$

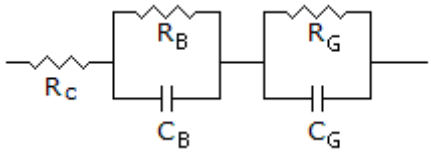

Fig. 2.14: Parallel RC circuit with grain boundary effects included. R_G and C_G represent grain boundary resistance and capacitance, while R_B and C_B represent bulk resistance and capacitance.

This circuit has an impedance Nyquist plot as shown in Fig. 2.15. If the grain boundary arc is large enough, it is possible that the bulk arc will only occur at frequencies above the range of the lab equipment, and will therefore be completely obscured.

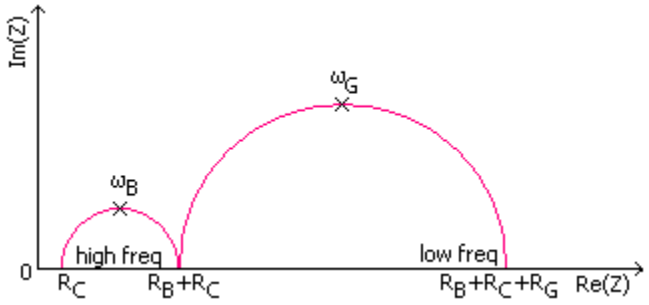

Fig. 2.15: Nyquist plot of the complex impedance for the circuit shown in Fig. 2.14.

Some examples of Nyquist plots for different R and C values are shown in Fig. 2.16. It is worthwhile to note that the arcs will only have well defined intercepts and therefore extractable values for R and C if certain conditions are met.

First, for the center of the arcs (located at the resonant frequency for each phase) to be separate and to prevent overlap at the $R_B + R_C$ intercept, C_B and C_G must differ by several orders of magnitude (more specifically, the actual limit depends on the R values). If C_G and C_B are equal, the arcs will combine into one large arc, as shown below.

Second, the range of frequencies applied must great enough so that the R_C intercept is well defined – i.e. ω must effectively approach infinity. This second condition is the most difficult to deal with experimentally, because the range of our frequency sweeper extends to just over 5MHz. In the plots below, this experimental limit is used, and many of the arcs are therefore incomplete. Indeed, it is possible that the smaller resistivity of the bulk material (grain interior) could cause the bulk arc to be lost completely inside the gap.

It is still possible to determine the bulk resistance and capacitance from an impedance spectrum dominated by grain boundary effects. In this case, we should be able to use equation 2.8 to determine the bulk capacitance from the boundary capacitance. With negligible contact resistance, we should also be able to determine the resistance of the bulk by using a fitting program to determine the R_B intercept.

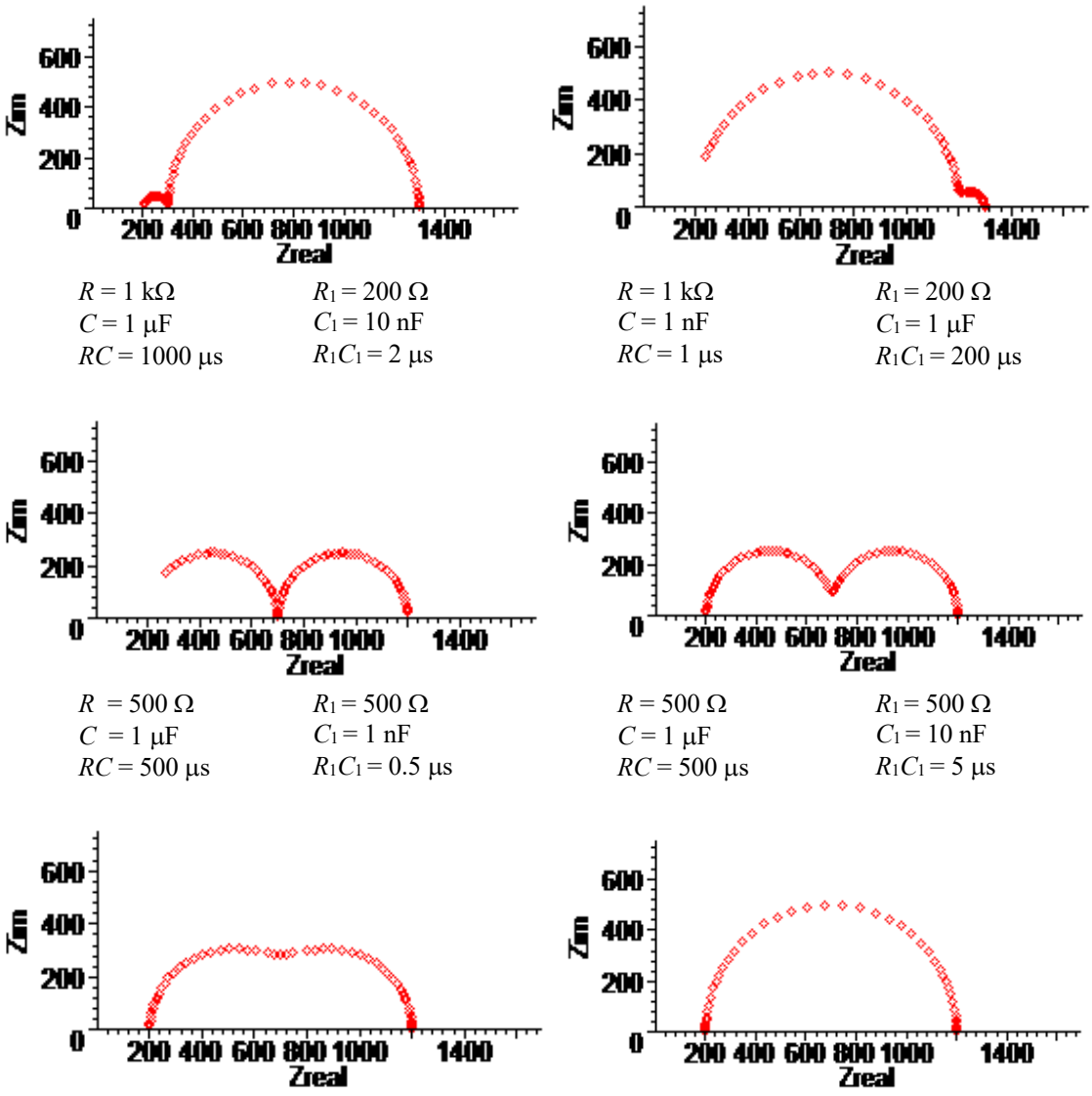

R = 1 kΩ	R_1 = 200 Ω	R = 1 kΩ	R_1 = 200 Ω
C = 1 μF	C_1 = 10 nF	C = 1 nF	C_1 = 1 μF
RC = 1000 μs	R_1C_1 = 2 μs	RC = 1 μs	R_1C_1 = 200 μs
R = 500 Ω	R_1 = 500 Ω	R = 500 Ω	R_1 = 500 Ω
C = 1 μF	C_1 = 1 nF	C = 1 μF	C_1 = 10 nF
RC = 500 μs	R_1C_1 = 0.5 μs	RC = 500 μs	R_1C_1 = 5 μs
R = 500 Ω	R_1 = 500 Ω	R = 500 Ω	R_1 = 500 Ω
C = 100 nF	C_1 = 1 nF	C = 100 nF	C_1= 100 nF
RC = 50 μs	R_1C_1 = 0.5 μs	RC = 50 μs	R_1C_1 = 50 μs

Fig. 2.16: Nyquist plots for various component values in two series R//C circuits, within the frequency range of our equipment (10Hz-5MHz). For all: R_C = 200Ω.

3 Samples

Our samples are compressed powders of $BaCuS_{1-x}Se_xF$ compounds, in steps of x=0.00, 0.25, 0.50, and 0.75. The samples are cylindrical pellets, of average diameter 6mm and average height 3mm. The density of the pellets is approximately 5 g/cm^3, or approximately 15% less dense than a solid crystal of the same material.

The powder was prepared by mixing stoichiometric proportions of BaF_2, $BaCu_2S_2$, and $BaCu_2Se_2$. Synthesis was achieved by heating the materials in an evacuated silica tube at 650 ^oC for 15 hours.[6] The powder was then pressed into pellets as described above.

The interest in these materials stems from their potential to serve as transparent, p-type conductors[10]. Also, BaCuSF emits visible light at orange wavelengths under ultra-violet stimulus. Doping with different elements changes the wavelength of the emitted light.

3.1 Expected Resistivity and Dielectric Constant Values for $BaCuS_{1-x}Se_{1-x}F$

Although $BaCuS_{1-x}Se_xF$ is a new material that lacks thorough cataloguing, we can obtain a reasonable range of expected values by looking at the values obtained for the grain interior and boundary resistivities and dielectric constant for similar materials.

Materials considered chemically similar to $BaCuS_{1-x}Se_xF$ include ITO, Cu, BaCuSF, $CuCrMgO_2$, $CuScO_2$, and $CuAlO_2$. Resistivities for these materials have an order of magnitude rage of 10^{-4} Ω cm for Cu to 10^0 Ω cm for $CuAlO_2$.

As for dielectric constants, most materials have a dielectric constant ranging from 1-100 times the permittivity of free space ($\varepsilon_0 = 8.8542 \times 10^{-12}$ F/m). More specifically, most semiconductors have a dielectric constant around 15 times the permittivity of free space. BaF_2 has a dielectric constant of approximately 7, while $BaSO_4$ has a dielectric constant of approximately 12.

As long as our obtained values are reasonable compared to these given values, they will be within accepted ranges.

4 Equipment

4.1 Hardware

The impedance spectroscopy experiment itself is relatively simple, and only requires basic analysis equipment. In our setup, the sample is inserted between two spring-loaded metallic contacts with diameters approximately twice those of the pellets. The contacts connect through a coaxial cable to a frequency sweeping voltage source. Our sweeper is a SI 1260 Schlumberger Impedance/Grain-Phase Analyzer, located in Gilbert Hall. We applied a frequency range of 10 Hz to 5MHz to our samples.

The source applies a user-defined voltage across the sample, and measures the magnitude of the current and its phase with respect to the voltage. The sweeping device then determines both components of the complex impedance from the data, and writes them to a data file

4.2 Software

The Analyzer is controlled by a QuickBasic program written by an unknown member of Dr. Art Sleight's research group. To view and fit the data to ideal circuit models, we used Scribner's *ZView* impedance arc analysis software, version 2.6 (demo).

4.3 Verification

To verify the Analyzer's output data, we ran several trials where some combination of off the shelf circuit components was connected directly to the setup. Plots of the data all appeared as expected. Fig. 5.1 shows one example of the data for our test circuits.

5 Experimental Results

5.1 A Note on Fitting Impedance Arcs

Impedance arcs are tricky functions to fit. As can be seen in Fig. 2.16, changing the relative value of the capacitances or the RC time constant even slightly can cause big changes in the shape of the arc. Furthermore, most fitting routines require a good initial estimate of the component values. Unfortunately, the values of the capacitances are not obvious from the impedance spectrum – it takes quite a bit of guessing and checking to even find their order of magnitude. Likewise, the contact and grain interior resistances are often beyond the frequency range of the plot, and are difficult to estimate in this case. In these situations, it is possible to attain irresolvable errors effectively over 100%.

For example, take the fit shown in Fig. 5.1 of one of the off the shelf circuit component plots from section 4 – in this case a parallel RC circuit like that shown in figure 2.12. The fit looks good, but on closer inspection, the fit parameters are in error by 1-20%. The initial estimates of the components were several orders of magnitude different from the actual values, and a large error margin resulted (using the actual component values for initial guesses gives a fit error of less than 2%). 20% error would be sufficient for our purposes; however, the fitting program was unable to differentiate between a 0.1 nF capacitor and effectively zero. This presents a serious problem, as we expect C_{gi} to be on the order of 10^{-12}. Several of our samples exhibited such errors, especially with the grain interior capacitance. Component values where this was the case have been labeled as unknown.

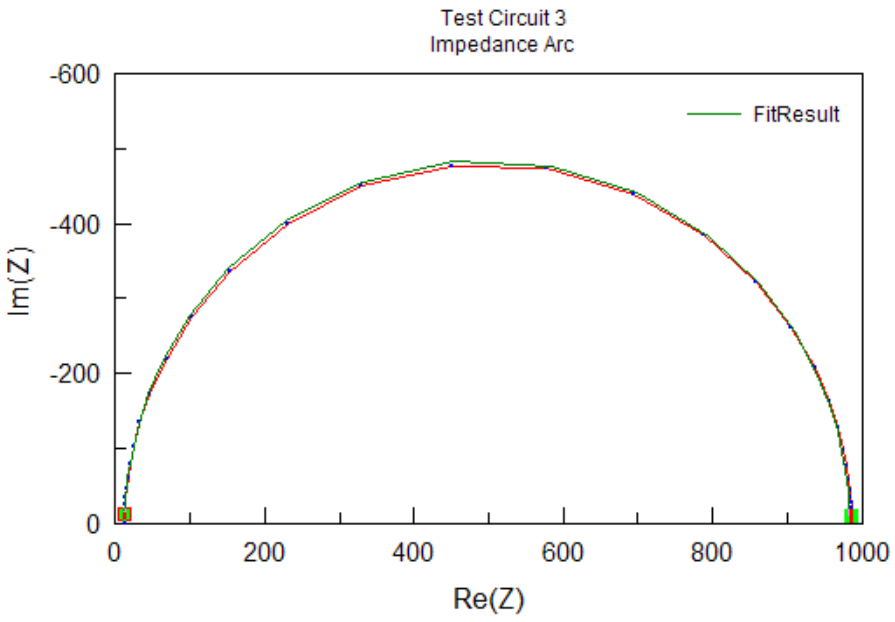

Test Circuit 3 Fit Parameters				
Component	Actual Value	Fit Value	Error	Error (%)
R_1	10 Ω	12.55 Ω	± 2.25 Ω	18.0 %
R_2	1000 Ω	970.6 Ω	± 20.6 Ω	2.13 %
C_1	0.1 nF	.00000000294 nF	± 4.32 nF	1.47e11 % (!)
C_2	10 nF	9.94 nF	± 0.32 nF	3.23 %

Fig. 5.1: Measured impedance arc and fitted arc for the test circuit shown in Fig. 5.2. Fit parameters are shown in the accompanying table.

5.2 Room Temperature Impedance Data

Our first goal was to obtain impedance spectra for each of the four samples at room temperature and constant applied voltage. We ran a minimum of three trials for each sample under these conditions. Averaged spectra and their best fits are shown on the following pages, Figs. 5.3-5.9

The model we chose to use for our samples is shown in Fig. 5.2, as derived in section 2.3.1.

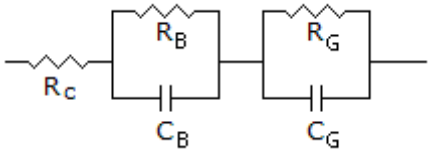

Fig. 5.2: Parallel RC circuit with grain boundary effects included. R_G and C_G represent grain boundary resistance and capacitance, while R_B and C_B represent bulk resistance and capacitance.

As per the problems discussed in section 5.1, achieving fits that were pleasing to the eye did not guarantee accurate component values. In fact, only one sample of the four gave consistent results. Fig. 5.5 shows the data for this sample, $BaCuS_{0.75}Se_{0.25}F$. The spectrum clearly is composed of at least two arcs, emphasized by the fit. Furthermore, the component values extracted from this spectrum have consistently small errors.

Unfortunately, the spectra of the other three samples did not extend to high enough frequencies to see such well-defined arcs. The fits for these spectra were not able to find an accurate value of the grain interior capacitance, and so were inaccurate for all the components. To compensate for this, we ran the fit again for one parallel RC circuit instead of two, as shown in Fig. 5.3. This gives us a way to check the value for R_{gb} and C_{gb} given by the double RC model. In the following data, all samples except $BaCuS_{0.75}Se_{0.25}F$ are fitted to both models.

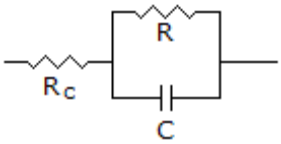

Fig. 5.3: Parallel RC circuit in series with contact resistance.

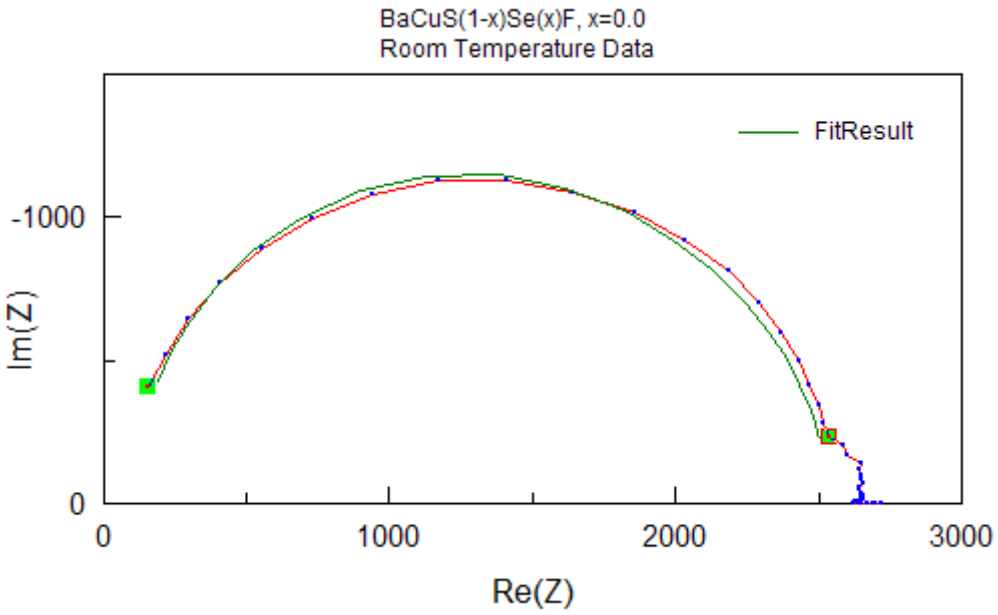

BaCuSF Room Temperature Fit Parameters		
Component	Fit Value	Error
$R_C + R_{gi}$	105 Ω	± 7.20 Ω
R_{gb}	2390 Ω	± 1.56 Ω
C_{gi}	?	n/a
C_{gb}	70 pF	± 1.10 pF

Fig. 5.4: Data and corresponding fit to the circuit shown in Fig. 5.3 for 1 volt applied to BaCuSF at room temperature.

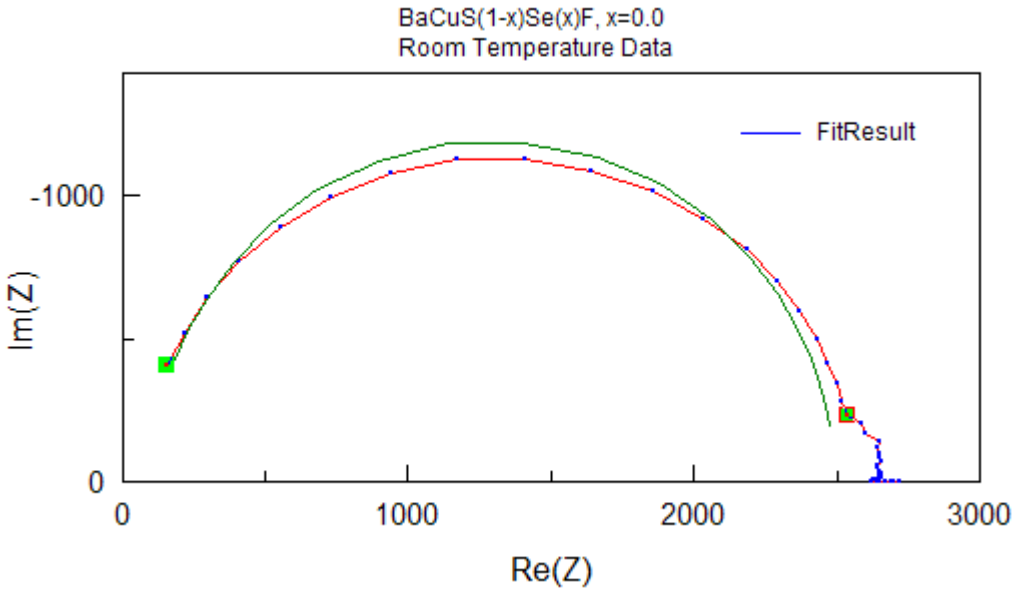

BaCuSF Room Temperature Fit Parameters		
Component	Software Fit	Error
R_C	107 Ω	± 7.20 Ω
R_{gi}	273 Ω	± 183 Ω
R_{gb}	2156 Ω	± 190 Ω
C_{gi}	?	n/a
C_{gb}	73.9 pF	± 3.27 pF

Fig. 5.5: Data and corresponding fit to the circuit shown in Fig. 5.2 for 1 volt applied to BaCuSF at room temperature.

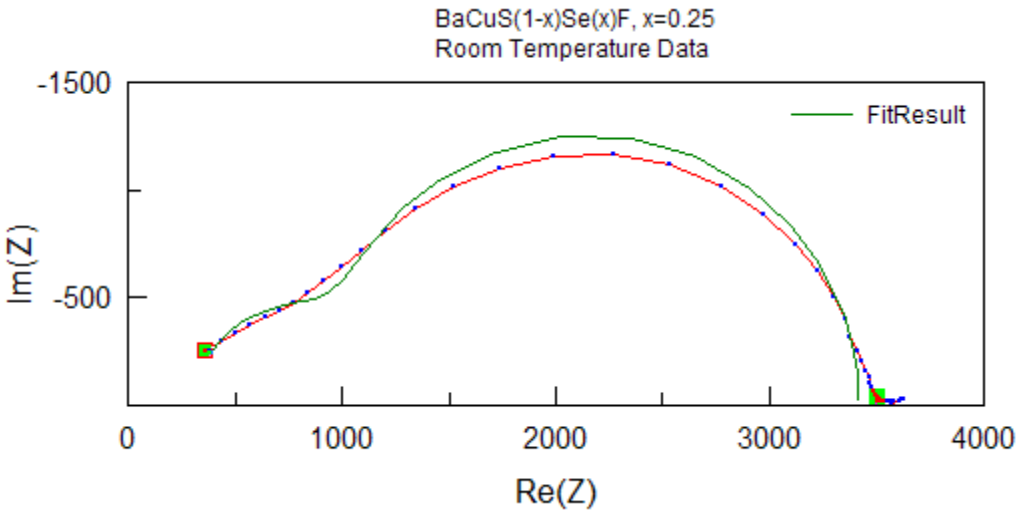

$BaCuS_{0.75}Se_{0.25}F$ Room Temperature Fit Parameters		
Component	Fit Value	Error
R_C	317 Ω	± 9.32 Ω
R_{gi}	648 Ω	± 15.0 Ω
R_{gb}	2453 Ω	± 24.6 Ω
C_{gi}	148 pF	± 5.42 pF
C_{gb}	824 pF	± 20.4 pF

Fig. 5.6: Data and corresponding fit to the circuit shown in Fig. 5.2 for 1 volt applied to $BaCuS_{0.75}Se_{0.25}F$ at room temperature.

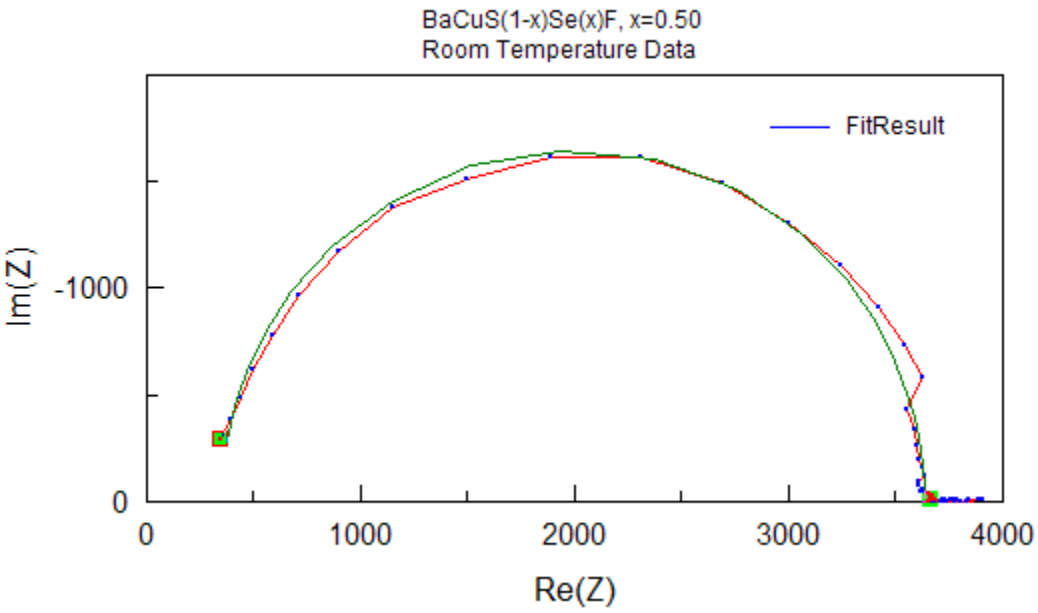

$BaCuS_{0.5}Se_{0.5}F$ Room Temperature Fit Parameters		
Component	Fit Value	Error
$R_C + R_{gi}$	372 Ω	± 7.39 Ω
R_{gb}	2290 Ω	± 9.72 Ω
C_{gi}	?	n/a
C_{gb}	90.8 pF	± 0.91 pF

Fig. 5.7: Data and corresponding fit to the circuit shown in Fig. 5.3 for 1 volt applied to $BaCuS_{0.5}Se_{0.5}F$ at room temperature.

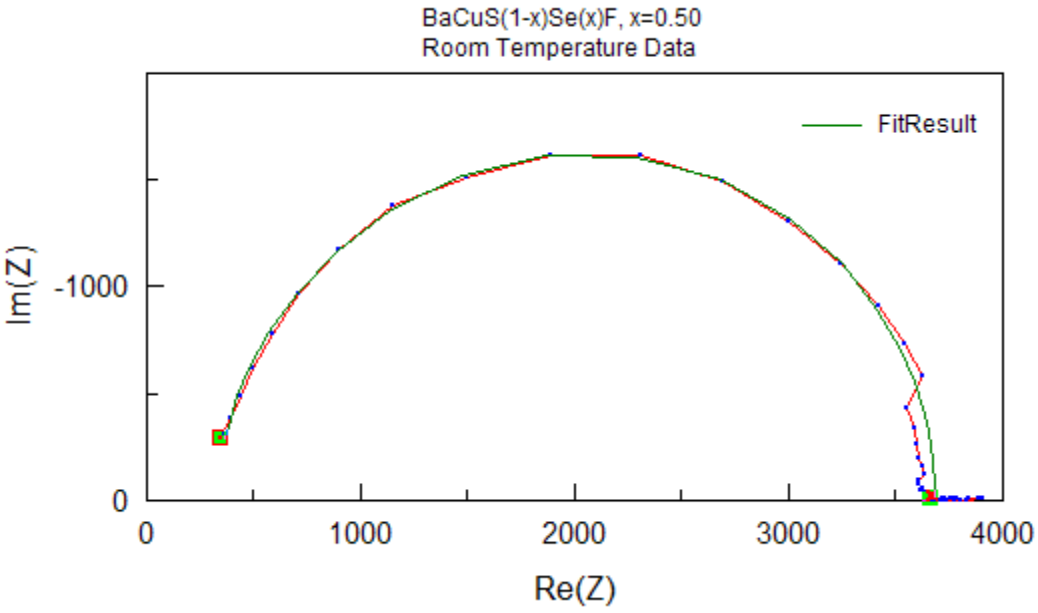

$BaCuS_{0.5}Se_{0.5}F$ Room Temperature Fit Parameters		
Component	Fit Value	Error
R_C	366 Ω	± 10.5 Ω
R_{gi}	366 Ω	± 87.5 Ω
R_{gb}	2520 Ω	± 75.8 Ω
C_{gi}	119 pF	± 6.46 pF
C_{gb}	418 pF	± 55.0 pF

Fig. 5.8: Data and corresponding fit to the circuit shown in Fig. 5.2 for 1 volt applied to $BaCuS_{0.5}Se_{0.5}F$ at room temperature.

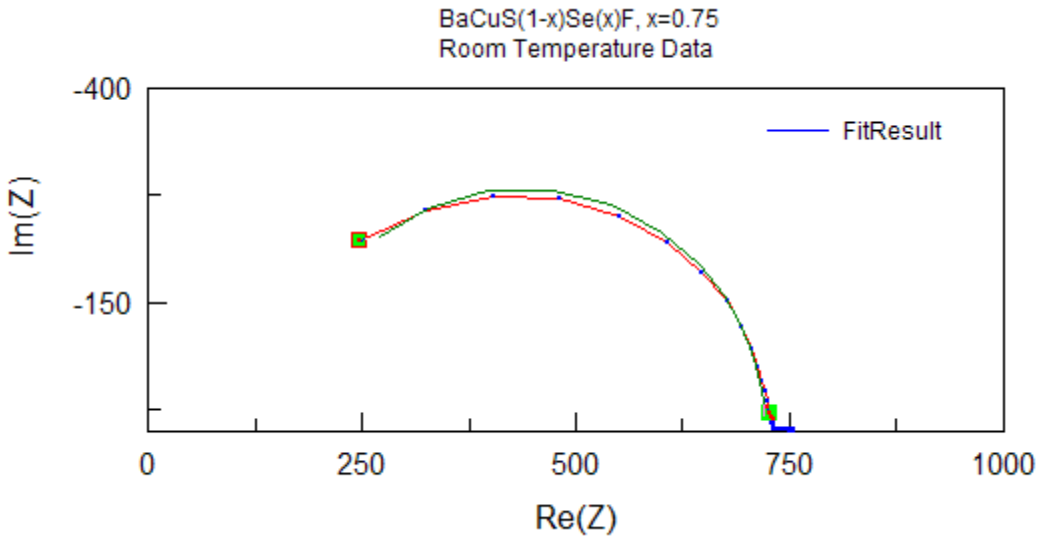

$BaCuS_{0.25}Se_{0.75}F$ Room Temperature Fit Parameters		
Component	Fit Value	Error
$R_C + R_{gi}$	182 Ω	± 2.70 Ω
R_{gb}	440 Ω	± 5.00 Ω
C_{gi}	?	n/a
C_{gb}	251 pF	± 15.9 pF

Fig. 5.9: Data and corresponding fit to the circuit shown in Fig. 5.3 for 1 volt applied to $BaCuS_{0.25}Se_{0.75}F$ at room temperature.

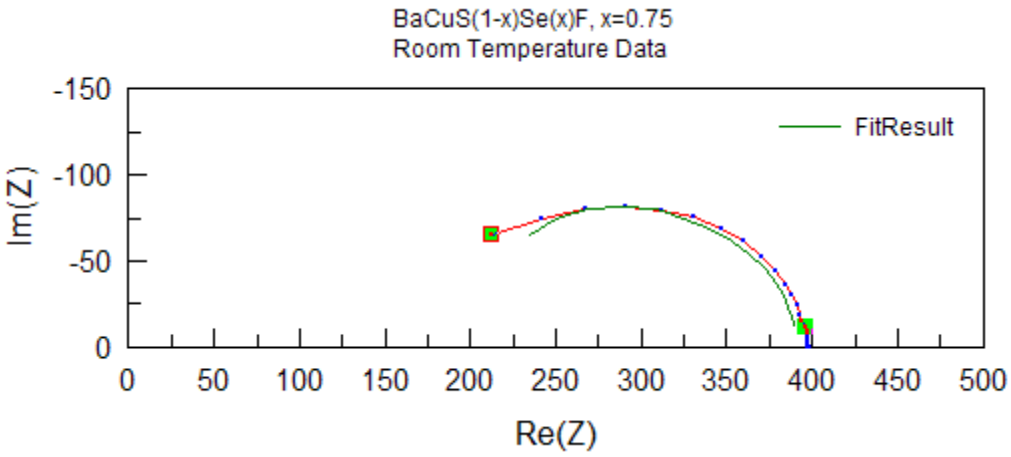

$BaCuS_{0.25}Se_{0.75}F$ Room Temperature Fit Parameters		
Component	Fit Value	Error
R_C	190 Ω	± 5.40 Ω
R_{gi}	53.1 Ω	± 8.20 Ω
R_{gb}	136.5 Ω	± 6.71 Ω
C_{gi}	?	n/a
C_{gb}	420.5 pF	± 14.0 pF

Fig. 5.9: Data and corresponding fit to the circuit shown in Fig. 5.2 for 1 volt applied to $BaCuS_{0.25}Se_{0.75}F$ at room temperature.

5.2.1 Sample Resistivities

In summary, the bulk resistances of the four samples are shown in Fig. 5.10. Using equation 2.3 and the samples' dimensions as given in section 3, we can calculate the resistivities of the samples shown also in Fig. 5.10:

Sample	Bulk Resistance	Resistivity
BaCuSF	270 ± 183 Ω	254 ± 172 Ω cm
$BaCuS_{0.75}Se_{0.25}F$	648 ± 15.0 Ω	610 ± 14 Ω cm
$BaCuS_{0.50}Se_{0.50}F$	366 ± 87.5 Ω	344 ± 82 Ω cm
$BaCuS_{0.25}Se_{0.75}F$	53.1 ± 8.20 Ω	49 ± 7.5 Ω cm

Fig. 5.10: Measured sample resistances and their corresponding resistivities.

These resistivities are much higher than our proposed range of 10^{-5} to 10^{0} given in section 3.1. To check these results, we ran the samples through a Van der Pauw system[8,9], with the following results:

Sample	Resistivity
BaCuSF	0.977 Ω cm
$BaCuS_{0.75}Se_{0.25}F$	15.0 Ω cm
$BaCuS_{0.50}Se_{0.50}F$	6.70 Ω cm
$BaCuS_{0.25}Se_{0.75}F$	4.29 Ω cm

Fig. 5.11: Sample resistivity as determined through Van der Pauw measurements.

These results are one or two orders of magnitude lower than our calculations. the Van der Pauw measurement process is well developed and generally considered reliable. The only concern is that the thickness of the sample should be much less than its diameter[9], which is not the case for our samples. It is therefore possible that the resistivity measurements are in error, but even an error of 100% does not bring the results into agreement.

5.2.1 Sample Dielectric Constants

As discussed in section 5.1, we were unable to directly extrapolate the grain interior capacitances from the impedance spectra for most of the samples; however, we were able to extrapolate C_{gi} for $BaCuS_{0.75}Se_{0.25}F$. As expected from the derivation in 2.3.1, the correction factor between C_{gi} and C_{gb} is approximately 0.20. By knowing this correction factor and C_{gb}, we can estimate $C_{gi.}$ The bulk capacitances of the samples are shown in Fig. 5.12.

Sample	Boundary Capcitance	Bulk Capacitance
BaCuSF	73.9 ± 3.27 pF	14.8 ± 0.65 pF
$BaCuS_{0.75}Se_{0.25}F$	824 ± 20.4 pF	148 ± 5.42 pF
$BaCuS_{0.50}Se_{0.50}F$	418 ± 55.0 pF	119 ± 6.46 pF
$BaCuS_{0.25}Se_{0.75}F$	420 ± 14.0 pF	83.6 ± 2.8 pF

Fig. 5.12: Measured sample boundary capacitances and inferred bulk capacitances.

Experimentally determining a value for the *d/D* correction factor also allows us to calculate a value for the grain boundary depth *d*. With *d/D* = 0.20 and a typical grain size of 60 nm,[7] we find an approximate grain boundary depth of 12 nm, which is on the larger end of the proposed values. This could explain the dominant grain boundary effects we observed in the data.

Using equation 2.4 and the samples' dimensions given in section 3, we can calculate the dielectric constants of the samples, listed in Fig. 5.13. Taking the permittivity of free space to be 8.854 pF m^{-1}, we can also calculate the samples' relative dielectric constants:

Sample	Dielectric Constant	Rel. Dielectric Const.
BaCuSF	1560 ± 6.90 pF m^{-1}	176
$BaCuS_{0.75}Se_{0.25}F$	15600 ± 675 pF m^{-1}	1761
$BaCuS_{0.50}Se_{0.50}F$	14200 ± 675 pF m^{-1}	1603
$BaCuS_{0.25}Se_{0.75}F$	8870 ± 297 pF m^{-1}	1001

Fig. 5.13: Calculated sample dielectric constants, absolute and relative to ε_0.

These numbers are two orders of magnitude higher than we expected, similar to the effect of the resistivity. We still expect that the actual values for the dielectric constant and resistivity are lower than the values we calculated, and that these high values are due to the inaccuracy of the modeling, as discussed in section 5.1.

One other effect to consider when approaching these numbers is the frequency dependence of the dielectric constant, especially in polar materials. Values for the dielectric constants of most materials are given at visible wavelengths – much higher frequencies than we have applied in our experiments. It is possible that at higher frequencies, the dielectric constant would correspond to known values.

It is also possible that other effects are present, such as contact (blocking) capacitances, asymmetrical grains, or sample defects.

6 Conclusions

AC impedance spectroscopy is a technique that, with care, can be used to give information about bulk and grain boundary properties of many materials. The circuit must be carefully modeled, and an appropriate frequency range must be spanned to have useful data.

If powdered composites of these materials are used in AC circuits as proposed, then grain boundary effects could become the limiting factor for their range of use. We hope that this is an issue that can be reduced with further research, including applying AC impedance spectroscopy at much higher frequencies (Ghz range) to more accurately plot the grain interior arc, developing more accurate circuit fitting programs, and producing materials with thinner – or less influential – grain boundaries.

7 Acknowledgements

Many thanks are in order for the tremendous patience of Dr. Janet Tate, who remained enthusiastic through every frustrating data set I took and every wrong path I led myself down this year, and under whose guidance I managed to integrate a wealth of information. Thank you as well to all the members of the Physics TCO research group for their support and assistance throughout the year.

8 References

[1] W.I. Archer and R. D. Armstrong. "The Application of A.C. Impedance Methods to Solid Electrolytes." *Electrochemistry*. Cambridge: John Wiley and Sons, 1987, 152-202.

[2] A. J. Bard and L. R. Faulkner. *Electrochemical Methods: Fundamentals and Applications*. New York: John Wiley and Sons, 1980.

[3] J. R. Macdonald, *Impedance Spectroscopy: Emphasizing Solid Materials and Systems*. New York: John Wiley and Sons, 1987.

[4] N.M. Beekmans and L. Heyne. *Electrochim. Acta.* **21** (year) 303-310.

[5] B.G. Streetmank, and S. Banerjee. *Solid State Electronic Devices*. New Jersey: Prentice Hall, 2000.

[6] C. Park, D. A. Keszler, H. Yanagi, J. Tate. *Thin Solid Films*. **445** (2003) 288-293.

[7] J. Lee, *et al*. *Journal of Materials Research.* **10** (1995) 2295-2300.

[8] A. P. Schuetze, *et al*. *American Journal of Physics*. **72** (2004) 149-153.

[9] D. K. Schroder. *Semiconductor Material Device Characterization*. USA: Wiley-Interscience, 1998, 1-61.

[10] J. Tate, *et al*. *Journal of Solid State Chemistry.* **175 (**2003) 24-8.

[11] G.E. Pike, *et al*. *Journal of Applied Physics*. **57** (1985) 5512-5518.

[12] T. Takeuchi, *et al*. *Journal of the American Ceramics Society*. **77** (1994) 1665-1668.

[13] R. Einzinger. "Grain Boundary Phenomena in ZnO Varistors." *Grain Boundaries in Semiconductors: proceedings of the Materials Research Society annual meeting.* New York : North-Holland, 1982, 343-355.

[14] J. Tate, *et al. Thin Solid Films*. **411** (2002) 119-124.